

The Optics of the ELETTRA Transverse Profile Monitor

M. Ferianis, T. Monaci, R. Passini
Sincrotrone Trieste
Padriciano 99 - 34012 Trieste - Italy

Abstract

The ELETTRA Transverse Profile Monitor (called SRPM from Synchrotron Radiation Profile Monitor) is presented. The SRPM focuses the photon beam emitted by a low dispersion bending magnet port in order to evaluate the emittance of the stored electron beam. A CCD with UV coating is used to improve the resolution by reducing the diffraction error. All the functions of the SRPM are monitored and can be controlled from the control room, including the motion of the optical components. For small emittance and increasing energy of an electron storage ring, the design of a proper Transverse Profile Monitor becomes more difficult since the dimension of the beam becomes comparable with the diffraction pattern. The use of shorter wavelengths (in the UV range) is effective only as far as the shape errors of the optical surfaces are proportionally reduced. The tests performed on the SRPM confirmed the correctness of the choice of UV wavelengths and the use of top quality optical components. Analysis and test results are compared and presented here.

1. GENERAL DESCRIPTION

A special bending magnet port has been designed for the SRPM in order to select a source point having negligible dispersion [1]. In this way the measurement of the beam size leads directly to an evaluation of the beam emittance. The expected beam sizes at the source point are given in Tab.1.

Energy	1.5 GeV	2.0 GeV
σ_h	66 μm	87 μm
σ_v (10% coupling)	65 μm	87 μm
σ_v (1% coupling)	20 μm	27 μm

Table 1 Expected beam sizes.

The optical system is schematically described in Fig.1 and gives a magnification equal to 4. Fig.2 is a photograph of the vacuum chamber containing the first mirror and the diaphragm. The first mirror, specifically designed for this application, acts as X-ray absorber and it is a glidcop® substrate water cooled on one side and platinum coated on the other. The vacuum window as been studied for vacuum safety and top optical characteristics. All the transparent components have been made in quartz for UV operation. The slits, the second mirror, the attenuator and the CCD camera are motorised by means of stepper motors for remote control. The image detected by the CCD is acquired and analysed in real time. Attenuation, alignment correction and focusing are automatically controlled using the analysis results. Direct

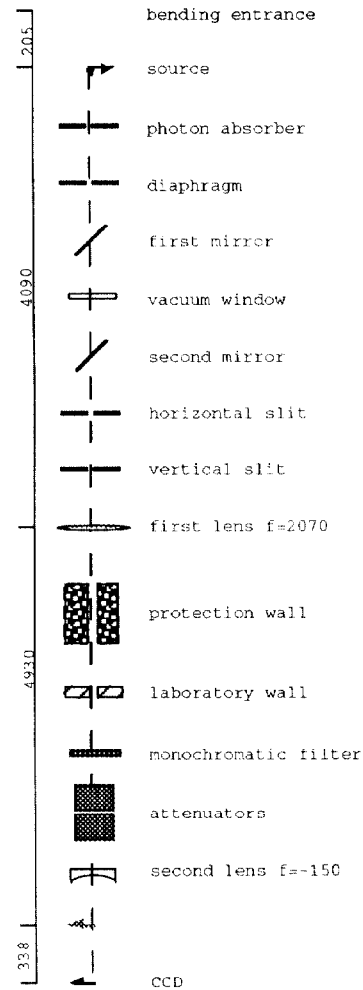


Figure 1 Optical system.

beam observation is available in Control Room on a dedicated monitor. Analysis results and software supervision are possible through Control System Link for full remote operation.

1.1. The alignment

The vacuum chamber has been aligned with the same procedure used for the magnets. First the optical centre of the chamber was found, then two Taylor spheres were positioned, and finally the chamber was connected to the bending port and aligned with the bending magnet.



Figure 2 Vacuum chamber and some optical components.

2. THE OPTICS

The image on the CCD is the convolution of the beam transverse distribution with the image produced by a single electron. To obtain a single electron image smaller than the beam size the attention has been focused on three main points: short wavelengths [2], top quality optics and X-ray interception. Furthermore, the theory of the radiation emission in a bending magnet needed to be reviewed and updated [3] to foresee exactly the single electron image. This image in fact can not be directly observed, but a good knowledge of it is important to calculate the source distribution from the image of the beam.

2.1. Theory update

The treatment of the depth of field found in the literature seems not to be accurate enough. The electron can not be considered as independent sources in different points along its trajectory. The emission by a single electron is in fact a coherent phenomenon. On the other hand, the commonly accepted bidimensional angular distribution does not contain any phase information or, in other words, does not describe the emitted wavefront. The method proposed is to calculate first the emitted wavefront and then, by a bidimensional Fourier transform, the single electron image, which contains implicitly the depth and the curvature of the source. An expression for the wavefront has been calculated [3] and is here presented. The electric field angular distribution can be written as

$$E(\varphi_x, \varphi_y, \lambda) = E(\lambda, \varphi_y) \cdot \chi(\varphi_x) e^{-i \frac{2\pi}{\lambda} \ell(\varphi_x, \varphi_y)} \quad (1)$$

where φ_x and φ_y are the horizontal and vertical angle referred to the electron velocity vector, and λ is the

wavelength. Considering only the component polarised parallel to the orbit plane, the first and the second term on the right can be expressed as

$$E(\lambda, \varphi_y) [\text{V} \cdot \text{m}^{-2}] = \frac{e}{\sqrt{6\pi^3 \epsilon_0} d} \left(\frac{R}{\lambda^3} \right) \left(\frac{1}{\gamma^2} + \varphi_y^2 \right) K_{2/3}(\xi)$$

and

$$\chi(\varphi_x) = \begin{cases} 1 & \text{for } -\varphi_x < \varphi_x < \varphi_x \\ 0 & \text{elsewhere} \end{cases}$$

where

- $K_{2/3}(\xi)$ is the modified Bessel function of order 2/3

- $\xi = \frac{R}{3\lambda} \left(\frac{1}{\gamma^2} + \varphi_y^2 \right)^{3/2}$

- $\gamma = \frac{1}{\sqrt{1 - \frac{v^2}{c^2}}}$

- e is the electron charge

- R is the radius of the electron orbit

- ϵ_0 is the dielectric constant in vacuum

- c is the light speed

- d is the distance from the source

Finally, the expression found for the distance between the wavefront and the reference sphere centred at the source point can be written as

$$\ell(\varphi_x, \varphi_y) \equiv \zeta(\varphi_x) - d - R\varphi_x - \frac{(\zeta(\varphi_x) - d) \cdot d}{2\zeta(\varphi_x)} \varphi_y^2 \quad (2)$$

with

$$\zeta(\varphi_x) = R \sin \varphi_x + \sqrt{d^2 - R^2(1 - \cos \varphi_x)^2} \quad (3)$$

Not big numerical differences are expected between this and other methods, but yet big enough to influence the calculation of the beam dimensions starting from the beam image. Furthermore, this approach had many conceptual consequences in the design of the SRPM.

2.2. Short wavelengths and top quality optics

It is commonly known that reducing the wavelength the resolution improves or, in other words, the single electron image becomes smaller. On the other hand the inaccuracy of the real optical surfaces spreads up the image. The use of shorter wavelength is effective only as far as the wavefront distortion (WFD) is proportionally reduced. The effect of the WFD cannot be precisely computed because the surface inaccuracy is a stochastic function, but it is known that the intensity at the centre of the single electron image is reduced by a factor [4]

$$i(\sigma_{\text{wfd}}) \equiv 1 - \left(\frac{2\pi}{\lambda} \right)^2 \sigma_{\text{wfd}}^2 \quad (4)$$

where σ_{wfd} is the r.m.s. of the WFD. Using a gaussian approximation for the single electron image, Eq. (4) and

energy conservation can be satisfied only broadening the gaussian by a factor $i(\sigma_{\text{wid}})^{-1}$. In this way the WFD produced by the real optics can be taken into consideration designing a Transverse Profile Monitor. For the SRPM optics the global wavefront distortion has been specified less than $\lambda/4$ with $\lambda=250$ nm. Once found the manufacturers for such special components, it was necessary to test their compliance with the specifications. The method used to do it was to measure the whole optical system in diffraction limited operation. A small and intense coherent ultraviolet point-like source was made in the ICS/ICTP Laser Laboratory (Trieste, Italy) by launching the third harmonic of a Nd YAG laser into a monomode optical fibre [5]. The effect of the surface inaccuracy was directly observed by comparing the actual diffraction pattern produced by a defined aperture with the theoretical one. With the same method it was also possible to optimise the position of attenuators and filters, to measure the off axis aberration and in general to verify the correctness of the optical design.

2.3. X-ray interception

The first mirror is the most critical component in this kind of instrument. Besides the unavoidable finite flatness of the reflective surface, it presents a deformation due to the X-ray absorption, which heats the mirror mainly in a narrow horizontal strip as shown in Fig. 3.

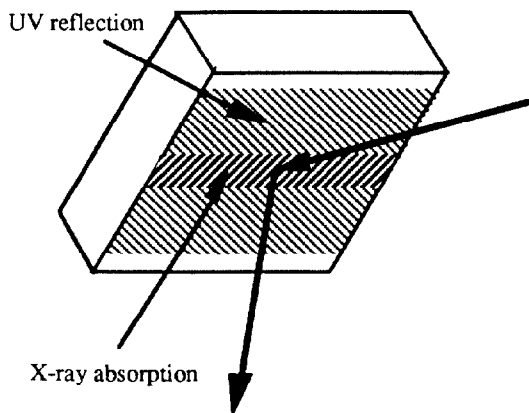


Figure 3 X-ray and UV distribution on the mirror surface

The heat distribution and the consequent deformation have been simulated [6] and the results compared with experimental observations. The effect is negligible for energies up to 1.5GeV and current of 200mA, but at 2.0GeV the image splits up in two separated spots. A different approach to the X-ray absorption has been proposed for the SRPM. Being the UV angular distribution wider than the X-ray distribution, a thin cooled bar can be used to intercept the most energetic part of the emission. In this way the thermal load on the mirror is reduced by a factor of 10. The shadow produced in the UV distribution only slightly increases the vertical dimension of the single electron image. In doing so, the mirror deformation is avoided and a constant

imaging of the beam over the whole energy range of ELETTRA is possible. The cooling of the bar does not present any technical difficulty and by using a thermocouple positioned inside the bar a good alignment with the emitted radiation can be obtained and maintained.

3. FIRST RESULTS

The SRPM is now operating with wavelengths around 330nm. Temporarily half of the mirror is screened by the vertical slit to get a constant imaging of the beam in spite of the mirror deformation. Furthermore the quality of the mirror surface is lower then expected even without thermal load. The single electron image calculated for this operative condition can be approximated with a bidimensional gaussian distribution having

$$\sigma_x = 64\mu\text{m} \quad \text{and} \quad \sigma_y = 58\mu\text{m}$$

Experimental observations with different electron beams confirm this figures within 10% error. Operating at 250nm, with X-ray interception and a better machined mirror surface

$$\sigma_x = 35\mu\text{m} \quad \text{and} \quad \sigma_y = 29\mu\text{m}$$

will be easily achieved.

4. REFERENCES

- [1] M. Ferianis, M. Plesko, internal communication (Str Memo 21/92)
- [2] Elettra Conceptual Design, Sincrotrone Trieste, April 1989
- [3] R. Passini, "Resolution Of The Transverse Profile Monitor", Sincrotrone Trieste, ST/M-94/1, March 1994
- [4] M. Born, E. Wolf, "Principles of Optics", Pergamon Press, 1989.
- [5] P. Apai, M. Berta, R. Passini, "Test On The Optics Of A Profile Monitor For Third Generation Synchrotron", to be published
- [6] A. Gambitta, internal communication